Renoprotective Effects of Laxative Linaclotide: Inhibition of Acute Kidney Injury and Fibrosis in a Rat Model of Renal Ischemia-Reperfusion

Yukihiro Hitaka[a,b], Naohito Isoyama[a], Shunya Tsuji[b,*] , Takeshi Honda[b, #], Yuki Nakayama[a], Mitsuhiro Yamaguchi[a], Kimihiko Nakamura[a], Hiroshi Hirata[a], Koji Shiraishi[a], and Masataka Asagiri[b,*]

[a]Department of Urology, Graduate School of Medicine, Yamaguchi University, 1-1-1 Minami-Kogushi, Ube, Yamaguchi 755-8505, Japan.
[b]Department of Pharmacology, Yamaguchi University Graduate School of Medicine, 1-1-1 Minami-Kogushi , Ube, Yamaguchi 755-8505, Japan.
#Present address: Department of Chemistry, Kurume University School of Medicine, Kurume, Fukuoka 830-0011, Japan

[*]**Corresponding**
Masataka ASAGIRI, Ph.D., M.H.Sc.
Department of Pharmacology
Graduate School of Medicine
Yamaguchi University
1-1-1 Minami-Kogushi, Ube, Japan
Tel: +81-836-22-2217; Fax: -2321
Email: masagiri@yamaguchi-u.ac.jp

Highlights

- Linaclotide mitigates kidney injury and fibrosis following I/R in a rat model
- Linaclotide diminishes macrophage activity in the acute phase of renal I/R injury
- The renoprotective effects of Linaclotide open avenues for its clinical repurposing

Abbreviations

Ischemia-reperfusion (I/R)
Chronic kidney disease (CKD)
Acute kidney injury (AKI)

Abstract

Ischemia-reperfusion (I/R) leads to tissue damage in transplanted kidneys, resulting in acute kidney injury (AKI) and chronic graft dysfunction, which critically compromises transplant outcomes, such as graft loss. Linaclotide, a guanylate cyclase C agonist clinically approved as a laxative, has recently been identified to exhibit renoprotective effects in a chronic kidney disease (CKD) model. This study evaluates the therapeutic effects of linaclotide on AKI triggered by I/R in a rat model with an initial comparison with other laxatives. Here, we show that linaclotide administration resulted in substantial reduction in serum creatinine levels, reflective of enhanced renal function. Histological examination revealed diminished tubular damage, and Sirius Red staining confirmed less collagen deposition, collectively indicating preserved structural integrity and mitigation of fibrosis. Further analysis demonstrated lowered expression of TGF-β and associated fibrotic markers, α-SMA, MMP2, and TIMP1, implicating the downregulation of the fibrogenic TGF-β pathway by linaclotide. Furthermore, one day after I/R insult, linaclotide profoundly diminished macrophage infiltration and suppressed critical pro-inflammatory cytokines such as TNF, IL-1β, and IL-6, signifying its potential to disrupt initial inflammatory mechanisms integral to AKI pathology. These findings suggest that linaclotide, with its established safety profile, could extend its benefits beyond gastrointestinal issues and potentially serve as a therapeutic intervention for organ transplantation. Additionally, it could provide immediate and practical insights into selecting laxatives for managing patients with AKI or CKD, regardless of the cause, and for those receiving dialysis or transplant therapy.

1. Introduction

The escalating prevalence of chronic kidney disease (CKD) [1] and the consequent increasing reliance on dialysis therapy have exerted a substantial financial burden on healthcare systems worldwide [2]. Renal transplantation, even in high-risk subpopulations such as the elderly and those with functional decline, offers improved quality of life, extension of patient survival, and a reduction in long-term healthcare expenditures compared to long-term dialysis [3-5]. Nevertheless, organ graft longevity remains a critical issue, with 5-year and 10-year graft survival rates for living donor kidney transplantation in the United States reported to be at 86.5% and 67.6%, respectively [6]; thus, there is a significant need for medical interventions that preserve or potentially enhance the long-term prognosis of organ grafts [7].

Ischemia-reperfusion (I/R) injury, characterized by the cessation and subsequent restoration of blood flow to an organ, is an adverse but intrinsic outcome of organ retrieval from donors and transplantation into recipients [7, 8]. This pathological condition is an unavoidable aspect of transplant surgery and has been reported to significantly compromise graft survival [7]. I/R injury initiates a cascade of complex pathophysiological processes, including both hypoxic and oxidative stress, cell

death, robust inflammatory responses, and tissue damage—all of which contribute substantially to acute kidney injury (AKI) in the transplanted graft [8, 9]. The inflammatory response in post-I/R AKI is substantially mediated by macrophage infiltration into the damaged tissue, leading to the secretion of pro-inflammatory cytokines such as IL-1β, IL-6, and TNF [8]. This triggers a sequence of events that recruits additional immune cells, thereby perpetuating and amplifying the inflammatory response [8], which in turn activates the TGF-β pathway, leading to collagen deposition and renal fibrosis [10, 11]. Since graft fibrosis is closely correlated with poor graft quality and causes graft failure [7], the reduction of I/R injury has emerged as a critical strategy in improving the long-term outlook for transplanted kidneys [7, 12].

Recent research has highlighted the pharmacological potential of linaclotide to protect kidney function in a mouse model of adenine-induced CKD [13], an intriguing discovery considering its primary clinical application as a guanylate cyclase C agonist laxative, even among patients receiving dialysis [14]. The recognized new pharmacological profile of linaclotide, in conjunction with its established clinical safety, has prompted us to investigate its potential protective effects on renal damage associated with transplant-related I/R injury using an animal model of I/R injury.

2. Materials and methods

2.1. Experimental animals and ischemia-reperfusion (I/R) models:

All animal experiments were approved by the Laboratory Animal Care Committee of the Yamaguchi University School of Medicine and conducted in accordance with the US National Institutes of Health Guidelines for the Management and Use of Laboratory Animals. Male Wistar rats (8-9 weeks old, 250-280 g, Kyudo, Saga, Japan) were housed in a room temperature of 25±1℃, and light (12-hour light/dark cycle) controlled environment. The rats were given standard chow and had access to water ad libitum.

For renal I/R model, rats were anaesthetized with isoflurane (3% induction, 1.5-2% maintenance) inhalation and placed on a heating pad to maintain a constant body temperature of 37 °C during surgery. The skin was then shaved, sterilized with 10% propidine-iodine and a median incision was made. To induce renal I/R injury, the left renal pedicle was clamped for 45 min, and then removed to reestablish blood circulation. The absence of blood flow during ischemia and the restoration of blood flow during reperfusion were assessed visually. Simultaneously nephrectomy of the right kidney was performed.

According to the experimental design, rats were euthanized 1 day or 14 days after reperfusion. Rats were randomly divided into sham, I/R and I/R + treatment groups (linaclotide: 100 μg/kg (Astellas, Tokyo, Japan), lubiprostone: 50 μg/kg (VIATRIS, Pennsylvania, United States) and sennoside: 24 μg/kg (Sawai, Osaka, Japan). Each drug was orally administered for consecutive 14 days before surgical operation. A day after surgery, each drug was orally administered until day 14. We considered day 1 after the operation as AKI, and day 14 as the transition phase from AKI to CKD [15].

2.2 Renal function assessment:

Blood samples were collected by intracardiac puncture and centrifuged (2,500 x g, 10 min). Serum creatinine was measured using a 7180 Clinical Analyzer (Hitachi, Tokyo, Japan). Serum creatinine levels provided an indicator of renal function and allowed evaluation of the effect of linaclotide on AKI/CKD and its potential for prevention.

2.3 Histopathological examination and immunohistochemical staining:

Kidney tissue was fixed in 4% paraformaldehyde over night at room temperature and embedded in paraffin. Three μm sections were used for all histological application. Hematoxylin-Eosin (Muto pure chemicals, Tokyo, Japan, 32048) staining was performed according to the manufacturer's protocol.

Tubular damage was assessed for tubular epithelial necrosis, tubular dilatation, loss of brush border and cast formation, according to the five-stage scoring system described below [16], with 10 damage quantifications in each section for each Hematoxylin-Eosin stained sample, graded in a blinded fashion by two examiners. 0 points: normal or none, 1 point: tubular damage ≤ 10%, 2 points: tubular damage 11-25%, 3 points: tubular damage 26-45%, 4 points: tubular damage 46-75%, 5 points: tubular damage ≥ 76%.

Sirius Red staining (picrosirius red stain kit, Polysciences, Inc., Warrington, PA, USA, 24901-250) staining was performed according to the manufacturer's protocols.

F4/80 staining was performed by using the following procedures. Briefly, sections were deparaffinized with xylene and rehydrated in graded alcohol. Endogenous peroxidase was blocked with 3% hydrogen peroxide for 10 min. Antigen retrieval was performed by using microwave in citrate buffer (pH 6.0). The sections were immunoblotted and incubated with primary antibody: F4/80 antibody (Proteintech, Wuhan, Hubei, China, 28463-1-AP, 1:4000) overnight at 4℃. The sections were then washed in PBS and incubated with secondary antibody (Histofine Simple Stain MAX PO, Nichirei, Tokyo, Japan, 424152) for 30 min at room temperature. The signal was detected by 3,3′ -diaminobenzidine (Nichirei, 415172) for 10 min. Sections were counterstained with Mayer's hematoxylin for 1 min and mounted.

Ten different and non-overlapping fields of view were randomly selected in each kidney section. To assess the degree of renal fibrosis and macrophage infiltration levels in each image, an automated quantification process was performed using the Hybrid Cell Counting application within the BZ-X analysis software (Keyence, Osaka, Japan, BZ-H4A).

2.4. Quantitative real-time PCR

Total RNA was extracted from kidney tissues was extracted using Trizol (Invitrogen, Carlsbad, CA, USA, 15596018) and RNeasy Plus Micro kit (Qiagen, Venlo, Netherlands, 74034) following the manufacturer's procedure. cDNA was generated using qScript cDNA Super Mix (QuantaBil, Massachusetts, USA, 95048). Quantitative real-time PCR assays were performed with SYBR Green Realtime PCR Master Mix (TaKaRa, Dalian, China, QPK-101) using Step One Plus PCR Systems

(Applied Biosystems, Foster City, CA, USA). *18S rRNA* was used as a control for gene expression analysis. Data was analyzed using the ΔΔCt method.

The specific primers are as follows;

18S rRNA:5'- CTC AAC ACG GGA AAC CTC AC-3' (forward) and 5'- CGC TCC ACC AAC TAA GAA CG-3' (reverse)

F4/80 (Adgre1) :5'-CTTTGGCTATGGGCTCCCAGTC-3' (forward) and 5'-CACGATCAACTCTGCCCTCCTTGC-3' (reverse);

Tgf-β：5'- ATA CGC CTG AGT GGC TGT CT-3'（forward) and 5'- TGG GAC TGA TCC CAT TGA TT-3'（reverse)

Tnf：5'- CTG AAC TTC GGG GTG ATC GG-3'（forward) and 5'- GGC TTG TCA CTC GAA TTT TGA GA-3'（reverse)

Il-1β：5'- GAA ATG CCA CCT TTT GAC AGT G-3'（forward) and 5'- TGG ATG CTC TCA TCA GGA CAG-3'（reverse)

Mmp2 :5'- ACC AAG AAC TTC CGA CTA TCC-3'(forward) and 5'- CTG AGC AAT GCC ATC AAA GAC-3'(reverse)

Timp1 :5'- TCC CCA GAA ATC ATC GAG AC-3'(forward) and 5'- TCA GAT TAT GCC AGG GAA CC-3'(reverse)

Collagen4a1 :5'- GTG TCA GCA ATT AGG CAG GTC AAG-3'(forward) and 5'- AGT CAG TCA TTC AGT CTG CGG ATA G-3'(reverse)

Il-6 :5'- CTG CAA GAG ACT TCC ATC CAG-3'(forward) and 5'- AGT GGT ATA GAC AGG TCT GTT GG-3'(reverse)

α-SMA:5'- CTA CAT GCG TCT GGA CTT GG-3'(forward) and 5'- CCA GGG AAG AAG AGG AAG CA-3'(reverse)

Collagen1a1 :5'- GCA AGA GGC GAG AGA GGT TT-3'(forward) and 5'- GAC CAC GGG CAC CAT CTT TA-3'(reverse)

2.5. Kidney hydroxyproline content

Kidney tissue was homogenized in ice-cold distilled water (900 μL) using a Power Gen homogenizer (Thermo Fisher Scientific, Massachusetts, USA, FS-PG125). Subsequently, 250 μL of 50% (wt/vol) trichloroacetic acid was added, and the homogenates were incubated further on ice for 2 hours. Precipitated pellets were hydrolyzed in 6 N HCl at 110 °C for 24 hours . After hydrolysis, the samples were filtered and neutralized with 10 N NaOH, and the hydrolysates were oxidized with Chloramine-T (Sigma Aldrich, St. Louis, USA, 857319) for 25 min at room temperature. The reaction mixture then was incubated in Ehrlich's perchloric acid solution at 65°C for 20 min and cooled to room temperature. The absorbance of the samples was measured at 560 nm in duplicate. Purified hydroxyproline (Sigma Aldrich, MAK008) was used to set a standard. Hydroxyproline content was expressed as nanograms of hydroxyproline per milligram of kidney.

2.6. 16S rRNA sequence and microbiome analysis

After 14 days I/R injury, microbial genomic DNA was extracted using QIAamp Fast DNA Stool Mini kit (Qiagen, Venlo, Netherlands, 51604) from rat feces. The V3-V4 region of 16S rRNA was amplified by using following primer pair. 16S amplicon Forward primer : TCGTCGGCAGCGTCAGATGTGTATAAGAGACAGCCTACGGGNGGCWGCAG, 16S amplicon Reverse primer : TCTCGTGGGCTCGGAGATGTGTATAAGAGACAGGACTACHVGGGTATCTAATCCA. Barcode and adaptor sequence were attached by Nextera XT Index Kit (Illumina). The 16S rRNA sequencing was performed by using a MiSeq sequencer (Illumina, San Diego, CA, USA). The sequence data was analyzed by BaseSpace (Illumina).

2.7. Statistics

All data are described as means ± standard deviation. Statistical analyses were performed by one-way ANOVA following Tukey's multiple comparisons test (Fig. 1B and D, Fig. 2A, C, and D, Fig. 3A, C, and D, Supplementary Fig. S1B, and Supplementary Fig. S2-4) and Log-rank (Mantel Cox) test (Fig. 1A) using GraphPad Prism software v 10.0 (GraphPad Software, San Diego, CA, USA). Statistical significance was set at $p < 0.05$.

3. Results:

3.1. Linaclotide reduces renal dysfunction in a rat model of I/R injury

Given the reported renoprotective effects of linaclotide [13] and lubiprostone [17] in an adenine-induced CKD model, we investigated the efficacy of these agents coupled with the stimulant laxative sennoside for ameliorating renal I/R injury a context relevant to post-transplantation AKI [18]. Our study showed that while sennoside and lubiprostone significantly reduced survival after I/R challenge, linaclotide did not adversely affect survival compared to the untreated I/R group (Figure 1A), suggesting a distinct renoprotective profile for linaclotide among the laxatives tested. Subsequent analysis of serum creatinine, a pivotal indicator of glomerular filtration function, revealed that linaclotide markedly lowered creatinine levels (Fig. 1B), suggesting preserved kidney function. Using Hematoxylin-Eosin staining for histomorphological assessment, we observed significant mitigation of renal tubular damage—a hallmark of renal pathology following I/R injury—in the linaclotide-treated animals (Fig. 1C). This protective effect was corroborated by a standardized damage scoring system (Fig. 1D), which aligning with the biochemical evidence of improved renal function. These findings imply that linaclotide can prevent the acute decline in renal function subsequent to I/R injury, offering a potential therapeutic avenue for managing AKI progression.

3.2. Linaclotide mitigates renal fibrosis during the late phase of post-I/R injury

Renal fibrosis is known to be associated with the development of CKD and graft failure [19]. We

subsequently assessed the impacts of linaclotide on the progression of fibrosis during the late phase of post-I/R injury. Investigation of the gene expression profile critical for fibrogenesis at 14 days post-I/R incident revealed a significant elevation in the mRNA levels of pro-fibrotic markers—such as *Collagen1a1*, *Collagen4a1*, *Tgf-β, α-SMA*, *Mmp2*, and *Timp1*—which were significantly attenuated by linaclotide treatment (Fig. 2A), elucidating its potential as a modulator of fibrogenic pathways. To complement these findings, we next analyzed physical alterations in tissue structure, i.e., deposition of collagen. Using Sirius Red staining, which is known to selectively label collagen fibers, we found that linaclotide markedly reduced collagen accumulation in kidney (Fig. 2B and C). Hydroxyproline assays supported these findings, revealing a reduction in total renal collagen content within the kidneys of linaclotide-treated animals 14 days post I/R incident (Fig. 2D). These results demonstrate that linaclotide prevents the development of renal fibrosis after I/R injury.

3.3. Linaclotide alleviates macrophage infiltration and inflammatory cytokine responses in the acute phase of post-I/R injury

Macrophage infiltration and inflammatory signaling during the initial phase post-I/R have implications for subsequent renal fibrosis [11]. Postulating that linaclotide may reduce macrophage-driven inflammatory events and thereby attenuate fibrosis, we examined the expression levels of macrophage marker *F4/80* (*Adgre1*) and pro-inflammatory cytokine genes (*Il-1β*, *Il-6*, and *Tnf*) within one day post-I/R injury (acute phase). We found that linaclotide significantly impaired these gene expression levels (Fig.3A). Immunohistochemical analysis using anti-F4/80 antibody confirmed a decrease in macrophage accumulation within the kidney in response to linaclotide treatment (Fig. 3B and C). Consistent with these results, serum creatinine concentrations were notably lower (Fig. 3D), and tubular damage was lessened (Supplementary Fig. S1A and B) in the linaclotide-treated group as opposed to the untreated control group. Altogether, our data present compelling evidence that linaclotide suppresses inflammation within the initial stages post-I/R injury and suggest its preemptive action against long-term fibrosis through modulation of macrophage infiltration and pro-inflammatory cytokine production in the renal milieu.

4. Discussion

In this study, linaclotide exhibited renoprotective effects in a rat model of I/R injury by attenuating macrophage infiltration and pro-inflammatory cytokine production in the kidney during the acute phase (one day post-I/R injury) and mitigating renal fibrosis in the later phase (14 days post-I/R injury). While previous studies have indicated that the laxatives lubiprostone and linaclotide may exert renoprotective effects by altering the gut microbiota, particularly *Clostridiales*, in a mouse model of adenine-induced CKD [13, 17], our initial findings show different results in our I/R-induced AKI model. Specifically, while lubiprostone and sennoside showed detrimental effects on survival after I/R

injury (Fig. 1A), linaclotide significantly alleviated the pathological features of AKI (Figs. 1-3 and Supplementary Fig. S1) without markedly altering the gut microbiota evidenced by our comprehensive analysis on day 14 after I/R injury (Supplementary Figs. S2-S4). Our data also revealed that, despite anticipated fluctuations in the gut microbiota composition, such as decreases in *Lactobacillus*, *Ruminococcaceae*, and *Lachnospiraceae* families—a trend consistent with reported dysbiosis following I/R injury [20, 21]—the administration of linaclotide did not lead to significant restoration or further detrimental shifts in these key microbial populations (Supplementary Figs. S2-S4). This unexpected result regarding gut microbiota suggests that changes in *Clostridiales*, previously linked to linaclotide's kidney protection, may not apply to our I/R-induced AKI model. Instead, this leads us to consider other pathways or mechanisms through which linaclotide could protect the kidney without significantly altering the gut microbes. Of course, the apparent discrepancies between these results could be attributed to differences in the animal models. Nevertheless, both the current study and the previous study [13] support the renoprotective effect of linaclotide, suggesting mechanisms other than regulation of the gut microbiota may underlie the beneficial effects of on kidney outcomes.

It has been well documented that renal fibrosis is promoted through TGF-β expression in fibroblasts, triggered by macrophage-derived IL-1β secretion [10]. In fact, both pharmacological [8] and genetic [11, 22] interventions targeting macrophage depletion have shown efficacy in ameliorating I/R injury, highlighting the therapeutic potential of modulating macrophage activity during the onset of AKI. In line with this, our research reveals that linaclotide significantly hinders macrophage infiltrations as well as the expression of inflammatory cytokines including IL-1β, IL-6, and TNF relatively initial phase of after I/R (one day post-I/R; Fig. 3A-D). Consistent with these results, we found a substantial reduction in TGF-β expression and subsequent renal fibrosis by linaclotide administration in the later phase of AKI (14 days post-I/R; Fig. 2A-D). Given the reported laxative effect of linaclotide as a guanylate cyclase C agonist acting on the apical surface of the intestinal tract to increase cGMP levels and its presumed low systemic bioavailability [23], it is postulated that the drug exerts renal effects indirectly. However, the exact mechanisms of how linaclotide acts pharmacokinetically in the body, where linaclotide first acts on cells, and affects macrophage infiltration in the context of renoprotection remain largely unclear and require further study. Nonetheless, our findings strongly indicate that mitigation of macrophage activity during the acute phase of renal I/R injury contributes significantly to the beneficial impact of linaclotide on I/R-induced AKI and subsequent renal fibrosis.

Previously, we have demonstrated that the suppression of inflammatory cytokines, such as TNF, during the acute phase of I/R can improve the long-term prognosis of kidney grafts [24-26]. Although various emerging therapeutic approaches, such as mesenchymal stem cell-derived extracellular vesicles [27], microRNAs [8], and toll-like receptor antagonists [8], show promise in ameliorating inflammatory responses triggered by I/R, they have yet to receive clinical approval. By

contrast, linaclotide has been deemed sufficiently safe for certain clinical applications, including dialysis. Our findings, therefore, elucidate the potential of linaclotide, beyond its established use for gastrointestinal disorders, as a promising candidate for drug repurposing in the management of I/R injury, particularly in the realm of kidney transplantation.

Figure legends

Figure 1. Linaclotide protects against renal ischemia-reperfusion (I/R) injury in male Wistar rats

Male Wistar rats (8-9 weeks old) were administrated linaclotide (100 μg/kg), sennoside (24 μg/kg), or lubiprostone (50 μg/kg) orally for 14 days prior to renal I/R injury; treatment resumed one day post-injury and continued until day 14 post-injury. (A) Kaplan–Meier survival curves for the following groups: Sham (n=6), I/R (n=9), I/R+Linaclotide (n=8), I/R+Sennoside (n=17), and I/R+Lubiprostone (n=16). (B) Serum creatinine levels (mg/dL) measured on day 14 post-I/R for Sham (n=6), I/R (n=6), and I/R+Linaclotide (n=6). (C) Hematoxylin-Eosin staining was used to assess renal tubular damage. Representative images of kidney samples (left six panels; scale bar = 200 μm or 100 μm, as indicated). Tubular damage was scored using a semi-quantitative scoring system ranging from 0 (normal) to 5 (≥76% damage; see the Materials and methods section for details: Sham (n=6), I/R (n=6), I/R+Linaclotide (n=6). Data are expressed as mean ± SD. Statistical significance was assessed by using Log-rank (Mantel Cox) test (for Fig. 1A) or by one-way ANOVA following Tukey's multiple comparisons test (for Fig. 1B and C). $^{*}P < 0.05$; $^{**}P < 0.01$; $^{***}P < 0.001$; $^{****}P < 0.0001$; n.s., not significant.

Figure 2. Linaclotide mitigates renal fibrosis induced by ischemia-reperfusion (I/R) injury

The effects of linaclotide on renal fibrosis were investigated at day 14 post-I/R injury. (A) RT-qPCR data showing relative expression levels of fibrosis markers (*Collagen1a1*, *Collagen4a1*, *Tgf-β*, *α-SMA*, *Mmp2*, and *Timp1*) normalized to sham expression levels set at 1. (B and C) Representative microscopic images of Sirius Red staining (Scale bars = 500 μm or 200 μm as indicated) (B), with corresponding quantitative analyses (C). (D) Hydroxyproline content, reflecting total collagen deposition in kidney samples, is shown. All graphs are expressed as mean ± SD for Sham (n=6), I/R (n=6), I/R+Linaclotide (Lina) (n=6). Statistical significance was assessed by using one-way ANOVA following Tukey's multiple comparisons test. $^{*}P < 0.05$, $^{**}P < 0.01$, $^{***}P < 0.001$, and $^{****}P < 0.0001$.

Figure 3. Linaclotide attenuates macrophage infiltration and inflammatory cytokine responses in initial phase of ischemia-reperfusion (I/R) injury

The acute-phase response to I/R injury was evaluated 24 h after I/R injury operation. (A) Kidney samples underwent RT-qPCR analysis. The relative gene expression levels of macrophage marker *F4/80* (*Adgre1*) and inflammatory cytokines (*Il-1β*, *Il-6*, and *Tnf*) normalized to the sham group set at

1. (B and C) Representative microscopic images for kidney infiltrating F4/80-positive macrophages (B: brown staining indicates cell-surface F4/80 antigen, scale bar = 100 μm) and F4/80-positive area was quantified using an automated method (C). (D) Serum creatinine concentrations. All results are expressed as mean ± SD: Sham (n=6), I/R (n=6), I/R+Linaclotide (Lina) (n=6). Statistical significance was assessed by one-way ANOVA following Tukey's multiple comparisons test. $^{*}P < 0.05$, $^{**}P < 0.01$, $^{***}P < 0.001$, and $^{****}P < 0.0001$.

Supplementary Figure S1.

Acute tubular pathology at 24 h post-ischemia-reperfusion (I/R) injury is alleviated by linaclotide

(A) Hematoxylin-Eosin staining is performed to assess renal tubular damage at 24 h after I/R injury operation. Scale bar = 200 μm or 100 μm. (B) Tubular damage was scored using a semi-quantitative scoring system on a scale from 0 (normal) to 5 (≥76% damage) (see the Materials and methods section for details). All results are expressed as mean ± SD: Sham (n=6), I/R (n=6), I/R+ Linaclotide (n=6). Statistical significance was assessed by one-way ANOVA following Tukey's multiple comparisons test. $^{*}P < 0.05$, $^{**}P < 0.01$, $^{***}P < 0.001$, and $^{****}P < 0.0001$.

Supplementary Figure S2.

The top 75 most common order taxa in the fecal microbiota

The y-axis indicates the abundance of each microbe (%). Control (n=6), I/R (n=6), I/R+ Linaclotide (n=6) in each group. Statistical significance was assessed by one-way ANOVA following Tukey's multiple comparisons test. $^{*}P < 0.05$, $^{**}P < 0.01$, and $^{****}P < 0.0001$.

Supplementary Figure S3.

The top 70 most common family taxa in the fecal microbiota

The y-axis indicates the abundance of each microbe (%). Control (n=6), I/R (n=6), I/R+ Linaclotide (n=6) in each group. Statistical significance was assessed by one-way ANOVA following Tukey's multiple comparisons test. $^{*}P < 0.05$, $^{**}P < 0.01$.

Supplementary Figure S4.

The top 60 most common genus taxa in the fecal microbiota

The y-axis indicates the abundance of each microbe (%). Control (n=6), I/R (n=6), I/R+ Linaclotide (n=6) in each group. Statistical significance was assessed by one-way ANOVA following Tukey's multiple comparisons test. $^{*}P < 0.05$, $^{**}P < 0.01$.

Funding

This work was supported by the Japan Society for the Promotion of Science (23K15250,

23K14085, 20K09412), Research Grant from the UBE Foundation, and FOCS grant from Yamaguchi University Graduate School of Medicine.

Author contributions

N.I. conceptualized this work; Y.H., T.H., Y.N. and M.Y. performed experiments and analyzed data; T.H., S.T., Y.N., K.N. and H.H. provided technical assistance; Y.H., N.I., T.H. and H.H. administered the project; Y.H., S.T. and M.A. wrote the manuscript; N.I. K.S. and M.A. supervised the project. All authors approved the final version of the manuscript.

Declaration of competing interest

From 2011 to 2016, MA was affiliated with the Innovation Center for Immunoregulation and Therapeutics, Graduate School of Medicine, Kyoto University, which was funded in part by Astellas Pharma Inc. The other authors declare that they have no apparent conflicting financial interests or personal relationships that could be perceived as influencing the results presented in this manuscript.

Acknowledgments

We thank Professor Kei Sakamoto (Department of Microbiology, Yamaguchi University Graduate School of Medicine) for insightful advice on fibrosis analysis.

Reference

[1] C. Hsu, Where Is the Epidemic in Kidney Disease?, Journal of the American Society of Nephrology. 21 (2010) 1607. https://doi.org/10.1681/ASN.2010050546.

[2] A. Roggeri, D.P. Roggeri, C. Zocchetti, M. Bersani, F. Conte, ReNe (Renal Lombardy Network), Additional contributors from ReNe Network, Healthcare costs of the progression of chronic kidney disease and different dialysis techniques estimated through administrative database analysis, J Nephrol. 30 (2017) 263–269. https://doi.org/10.1007/s40620-016-0291-8.

[3] P.P. Reese, J. Shults, R.D. Bloom, A. Mussell, M.N. Harhay, P. Abt, M. Levine, K.L. Johansen, J.T. Karlawish, H.I. Feldman, Functional Status, Time to Transplantation, and Survival Benefit of Kidney Transplantation Among Wait-Listed Candidates, Am J Kidney Dis. 66 (2015) 837–845. https://doi.org/10.1053/j.ajkd.2015.05.015.

[4] M. Tonelli, N. Wiebe, G. Knoll, A. Bello, S. Browne, D. Jadhav, S. Klarenbach, J. Gill, Systematic Review: Kidney Transplantation Compared With Dialysis in Clinically Relevant Outcomes, American Journal of Transplantation. 11 (2011) 2093–2109. https://doi.org/10.1111/j.1600-6143.2011.03686.x.

[5] D.M. Taylor, S.D.S. Fraser, J.A. Bradley, C. Bradley, H. Draper, W. Metcalfe, G.C. Oniscu,

C.R.V. Tomson, R. Ravanan, P.J. Roderick, A Systematic Review of the Prevalence and Associations of Limited Health Literacy in CKD, Clin J Am Soc Nephrol. 12 (2017) 1070–1084. https://doi.org/10.2215/CJN.12921216.

[6] E.D. Poggio, J.J. Augustine, S. Arrigain, D.C. Brennan, J.D. Schold, Long-term kidney transplant graft survival—Making progress when most needed, American Journal of Transplantation. 21 (2021) 2824–2832. https://doi.org/10.1111/ajt.16463.

[7] H. Zhao, A. Alam, A.P. Soo, A.J.T. George, D. Ma, Ischemia-Reperfusion Injury Reduces Long Term Renal Graft Survival: Mechanism and Beyond, EBioMedicine. 28 (2018) 31–42. https://doi.org/10.1016/j.ebiom.2018.01.025.

[8] H.K. Eltzschig, T. Eckle, Ischemia and reperfusion—from mechanism to translation, Nat Med. 17 (2011) 10.1038/nm.2507. https://doi.org/10.1038/nm.2507.

[9] R. Fuquay, B. Renner, L. Kulik, J.W. McCullough, C. Amura, D. Strassheim, R. Pelanda, R. Torres, J.M. Thurman, Renal Ischemia-Reperfusion Injury Amplifies the Humoral Immune Response, J Am Soc Nephrol. 24 (2013) 1063–1072. https://doi.org/10.1681/ASN.2012060560.

[10] S. Chung, J.M. Overstreet, Y. Li, Y. Wang, A. Niu, S. Wang, X. Fan, K. Sasaki, G.-N. Jin, S.N. Khodo, L. Gewin, M.-Z. Zhang, R.C. Harris, TGF-β promotes fibrosis after severe acute kidney injury by enhancing renal macrophage infiltration, JCI Insight. 3 (n.d.) e123563. https://doi.org/10.1172/jci.insight.123563.

[11] Macrophages: versatile players in renal inflammation and fibrosis | Nature Reviews Nephrology, (n.d.). https://www.nature.com/articles/s41581-019-0110-2 (accessed October 25, 2023).

[12] S.F. Smith, S.A. Hosgood, M.L. Nicholson, Ischemia-reperfusion injury in renal transplantation: 3 key signaling pathways in tubular epithelial cells, Kidney International. 95 (2019) 50–56. https://doi.org/10.1016/j.kint.2018.10.009.

[13] F. Nanto-Hara, Y. Kanemitsu, S. Fukuda, K. Kikuchi, K. Asaji, D. Saigusa, T. Iwasaki, H.-J. Ho, E. Mishima, T. Suzuki, C. Suzuki, T. Tsukimi, T. Matsuhashi, Y. Oikawa, Y. Akiyama, S. Kure, Y. Owada, Y. Tomioka, T. Soga, S. Ito, T. Abe, The guanylate cyclase C agonist linaclotide ameliorates the gut–cardio–renal axis in an adenine-induced mouse model of chronic kidney disease, Nephrology Dialysis Transplantation. 35 (2020) 250–264. https://doi.org/10.1093/ndt/gfz126.

[14] K. Sumida, A.A. Dashputre, P.K. Potukuchi, F. Thomas, Y. Obi, M.Z. Molnar, J.D. Gatwood, E. Streja, K. Kalantar-Zadeh, C.P. Kovesdy, Laxative use in patients with advanced chronic kidney disease transitioning to dialysis, Nephrol Dial Transplant. 36 (2020) 2018–2026. https://doi.org/10.1093/ndt/gfaa205.

[15] K. Minami, S. Bae, H. Uehara, C. Zhao, D. Lee, J. Iske, M.W. Fanger, J. Reder, I. Morrison, H. Azuma, A. Wiens, E. Van Keuren, B. Houser, A. El-Khal, P.M. Kang, S.G. Tullius, Targeting of intragraft reactive oxygen species by APP-103, a novel polymer product, mitigates ischemia/reperfusion injury and promotes the survival of renal transplants, Am J Transplant. 20 (2020)

1527–1537. https://doi.org/10.1111/ajt.15794.

[16] S. Song, X. Hou, W. Zhang, X. Liu, W. Wang, X. Wang, W. Cao, Y. Xia, W. Chen, C. Shi, Specific bFGF targeting of KIM-1 in ischemic kidneys protects against renal ischemia-reperfusion injury in rats, Regen Biomater. 9 (2022) rbac029. https://doi.org/10.1093/rb/rbac029.

[17] E. Mishima, S. Fukuda, H. Shima, A. Hirayama, Y. Akiyama, Y. Takeuchi, N.N. Fukuda, T. Suzuki, C. Suzuki, A. Yuri, K. Kikuchi, Y. Tomioka, S. Ito, T. Soga, T. Abe, Alteration of the Intestinal Environment by Lubiprostone Is Associated with Amelioration of Adenine-Induced CKD, J Am Soc Nephrol. 26 (2015) 1787–1794. https://doi.org/10.1681/ASN.2014060530.

[18] Z. Wang, Y. Cheng, W. Su, H. Zhang, C. Li, M.N. Routledge, Y. Gong, B. Qiao, Organ Specific Differences in Alteration of Aquaporin Expression in Rats Treated with Sennoside A, Senna Anthraquinones and Rhubarb Anthraquinones, Int J Mol Sci. 22 (2021) 8026. https://doi.org/10.3390/ijms22158026.

[19] M.A. Venkatachalam, J.M. Weinberg, W. Kriz, A.K. Bidani, Failed Tubule Recovery, AKI-CKD Transition, and Kidney Disease Progression, J Am Soc Nephrol. 26 (2015) 1765–1776. https://doi.org/10.1681/ASN.2015010006.

[20] J. Yang, C.J. Kim, Y.S. Go, H.Y. Lee, M.-G. Kim, S.W. Oh, W.Y. Cho, S.-H. Im, S.K. Jo, Intestinal microbiota control acute kidney injury severity by immune modulation, Kidney International. 98 (2020) 932–946. https://doi.org/10.1016/j.kint.2020.04.048.

[21] A. Huo, F. Wang, Berberine alleviates ischemia reperfusion injury induced AKI by regulation of intestinal microbiota and reducing intestinal inflammation, BMC Complementary Medicine and Therapies. 24 (2024) 66. https://doi.org/10.1186/s12906-023-04323-y.

[22] D.A. Ferenbach, J.V. Bonventre, Mechanisms of maladaptive repair after AKI leading to accelerated kidney ageing and CKD, Nat Rev Nephrol. 11 (2015) 264–276. https://doi.org/10.1038/nrneph.2015.3.

[23] J. Castro, A.M. Harrington, P.A. Hughes, C.M. Martin, P. Ge, C.M. Shea, H. Jin, S. Jacobson, G. Hannig, E. Mann, M.B. Cohen, J.E. MacDougall, B.J. Lavins, C.B. Kurtz, I. Silos-Santiago, J.M. Johnston, M.G. Currie, L.A. Blackshaw, S.M. Brierley, Linaclotide Inhibits Colonic Nociceptors and Relieves Abdominal Pain via Guanylate Cyclase-C and Extracellular Cyclic Guanosine 3′,5′-Monophosphate, Gastroenterology. 145 (2013) 1334-1346.e11. https://doi.org/10.1053/j.gastro.2013.08.017.

[24] N. Isoyama, P. Leurs, A.R. Qureshi, A. Bruchfeld, B. Anderstam, O. Heimburger, P. Bárány, P. Stenvinkel, B. Lindholm, Plasma S100A12 and soluble receptor of advanced glycation end product levels and mortality in chronic kidney disease Stage 5 patients, Nephrology Dialysis Transplantation. 30 (2015) 84–91. https://doi.org/10.1093/ndt/gfu259.

[25] Y. Nagata, M. Fujimoto, K. Nakamura, N. Isoyama, M. Matsumura, K. Fujikawa, K. Uchiyama, E. Takaki, R. Takii, A. Nakai, H. Matsuyama, Anti-TNF-α Agent Infliximab and

Splenectomy Are Protective Against Renal Ischemia-Reperfusion Injury, Transplantation. 100 (2016) 1675. https://doi.org/10.1097/TP.0000000000001222.

[26] Y. Nakayama, N. Isoyama, T. Yamamoto, Y. Nagata, M. Matsumura, K. Fujikawa, H. Matsuyama, K. Shiraishi, Receptor activator of the NFκB ligand system protects renal function during experimental renal ischemia-reperfusion in mice, Transplant Immunology. 58 (2020) 101263. https://doi.org/10.1016/j.trim.2020.101263.

[27] H. Hu, C. Zou, Mesenchymal Stem Cells in Renal Ischemia-Reperfusion Injury: Biological and Therapeutic Perspectives, Curr Stem Cell Res Ther. 12 (2017) 183–187. https://doi.org/10.2174/1574888X11666161024143640.

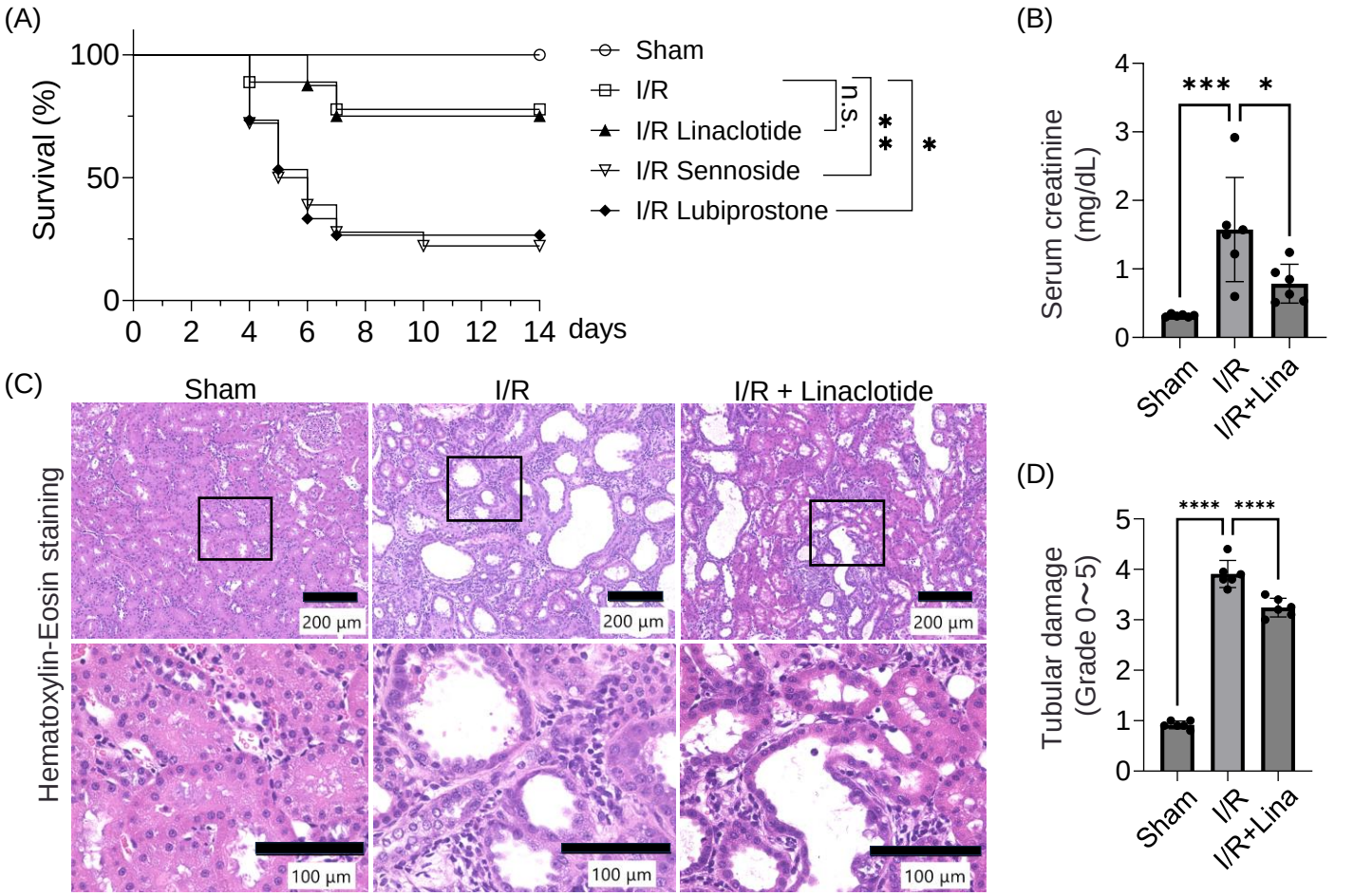
(A)
Survival (%)
100
50
0
0 2 4 6 8 10 12 14 days
Sham
I/R
I/R Linaclotide
I/R Sennoside
I/R Lubiprostone
n.s.
**
**
*
(B)
Serum creatinine (mg/dL)
4
3
2
1
0
***
*
Sham
I/R
I/R+Lina
(C)
Sham
I/R
I/R + Linaclotide
Hematoxylin-Eosin staining
200 μm
100 μm
(D)
Tubular damage (Grade 0~5)
5
4
3
2
1
0
****
****
Sham
I/R
I/R+Lina

Fig.1

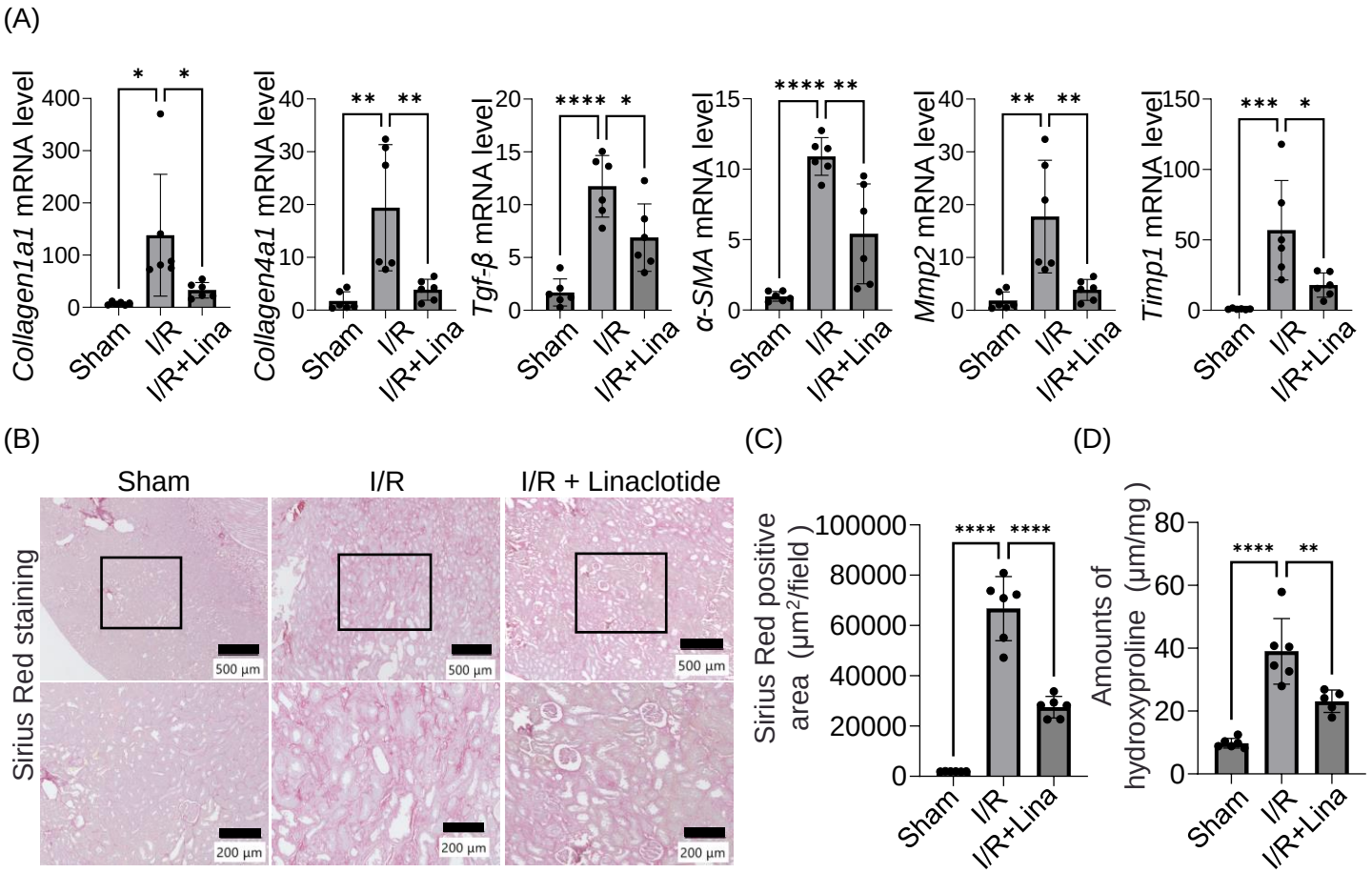
(A)
Collagen1a1 mRNA level
Collagen4a1 mRNA level
Tgf-β mRNA level
α-SMA mRNA level
Mmp2 mRNA level
Timp1 mRNA level
Sham
I/R
I/R+Lina
(B)
(C)
(D)
Sham
I/R
I/R + Linaclotide
Sirius Red staining
500 μm
200 μm
Sirius Red positive area (μm²/field)
Amounts of hydroxyproline (μm/mg)

Fig.2

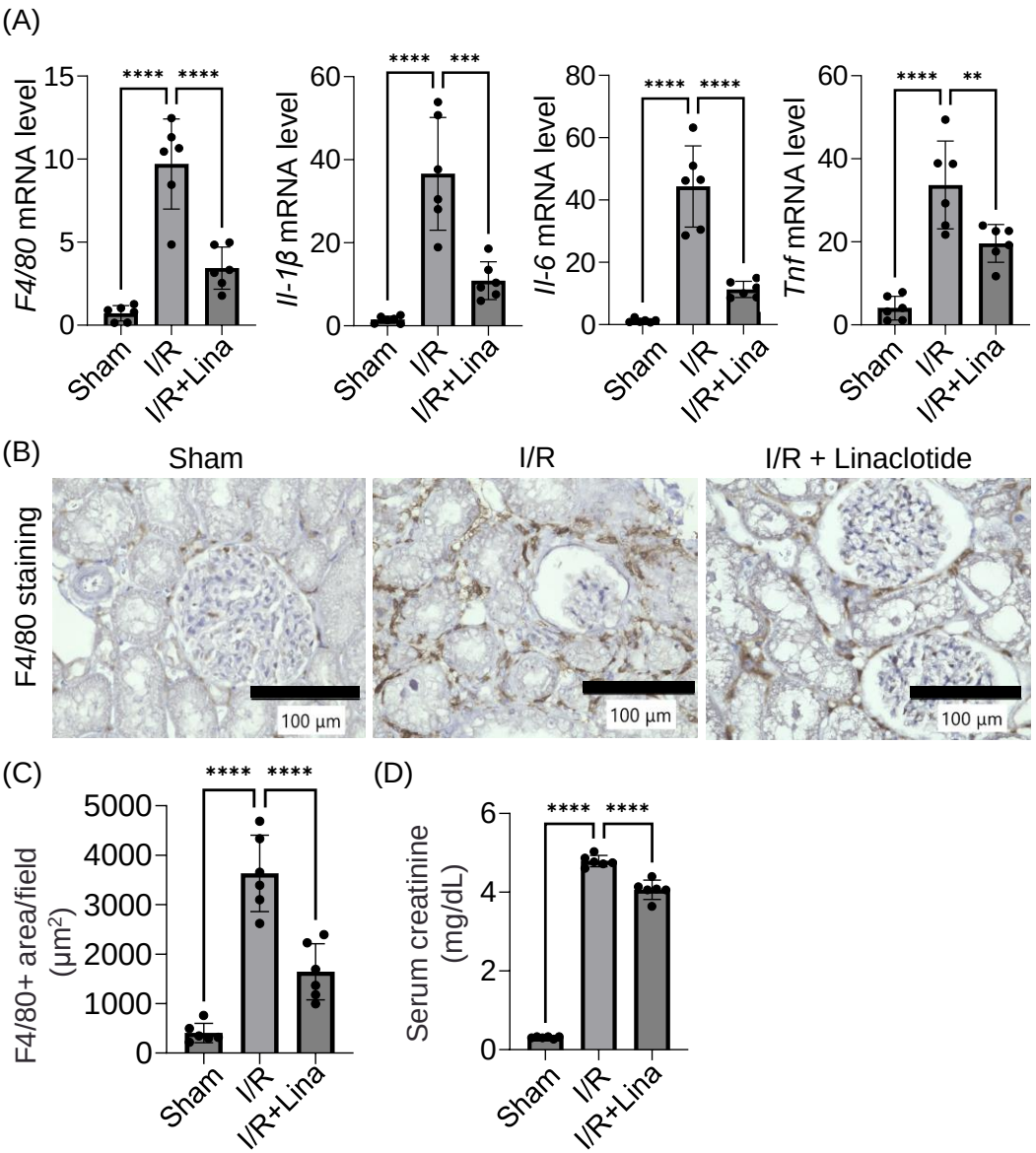
(A)
F4/80 mRNA level
Il-1β mRNA level
Il-6 mRNA level
Tnf mRNA level
Sham
I/R
I/R+Lina
(B)
Sham
I/R
I/R + Linaclotide
F4/80 staining
100 μm
(C)
F4/80+ area/field (μm²)
(D)
Serum creatinine (mg/dL)

Fig.3

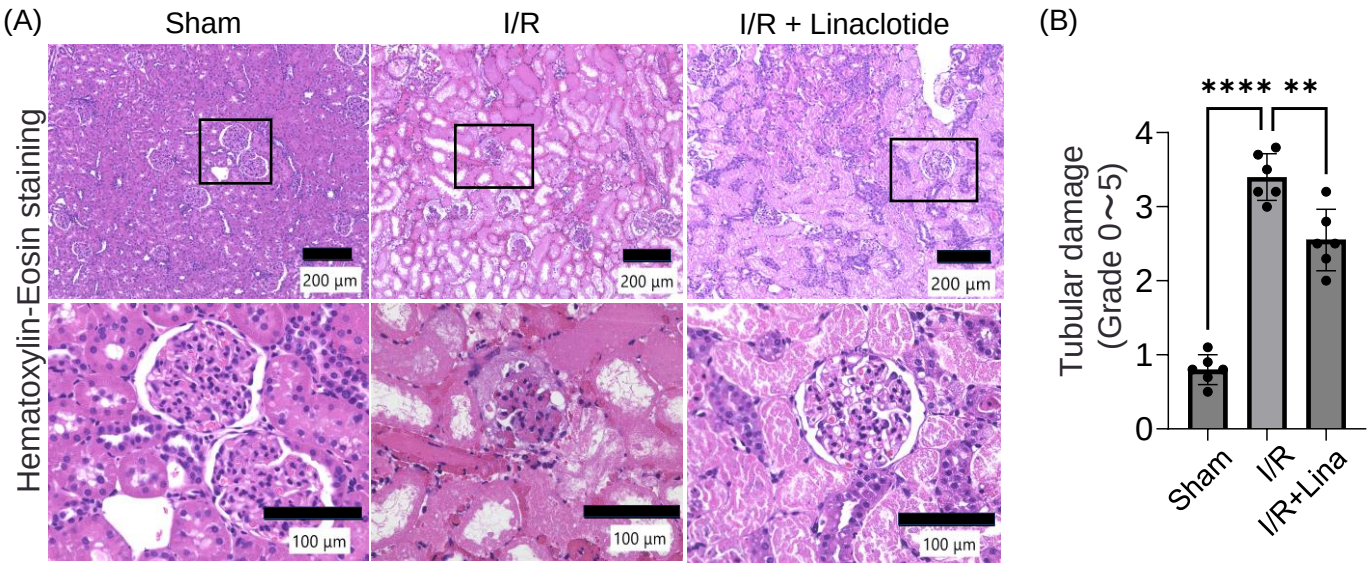

Supplementary Fig.1

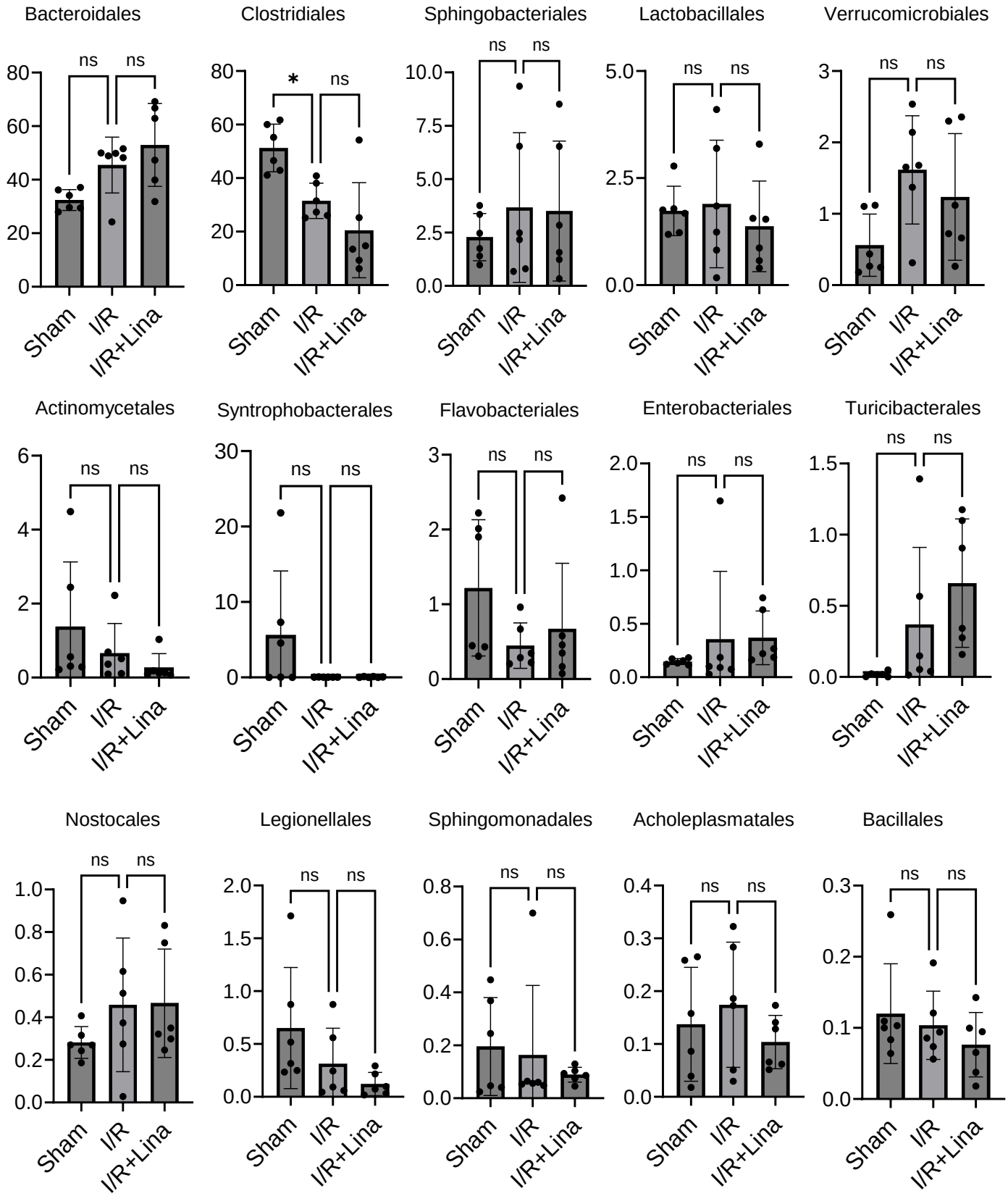

Supplementary Fig.S2
Order taxa

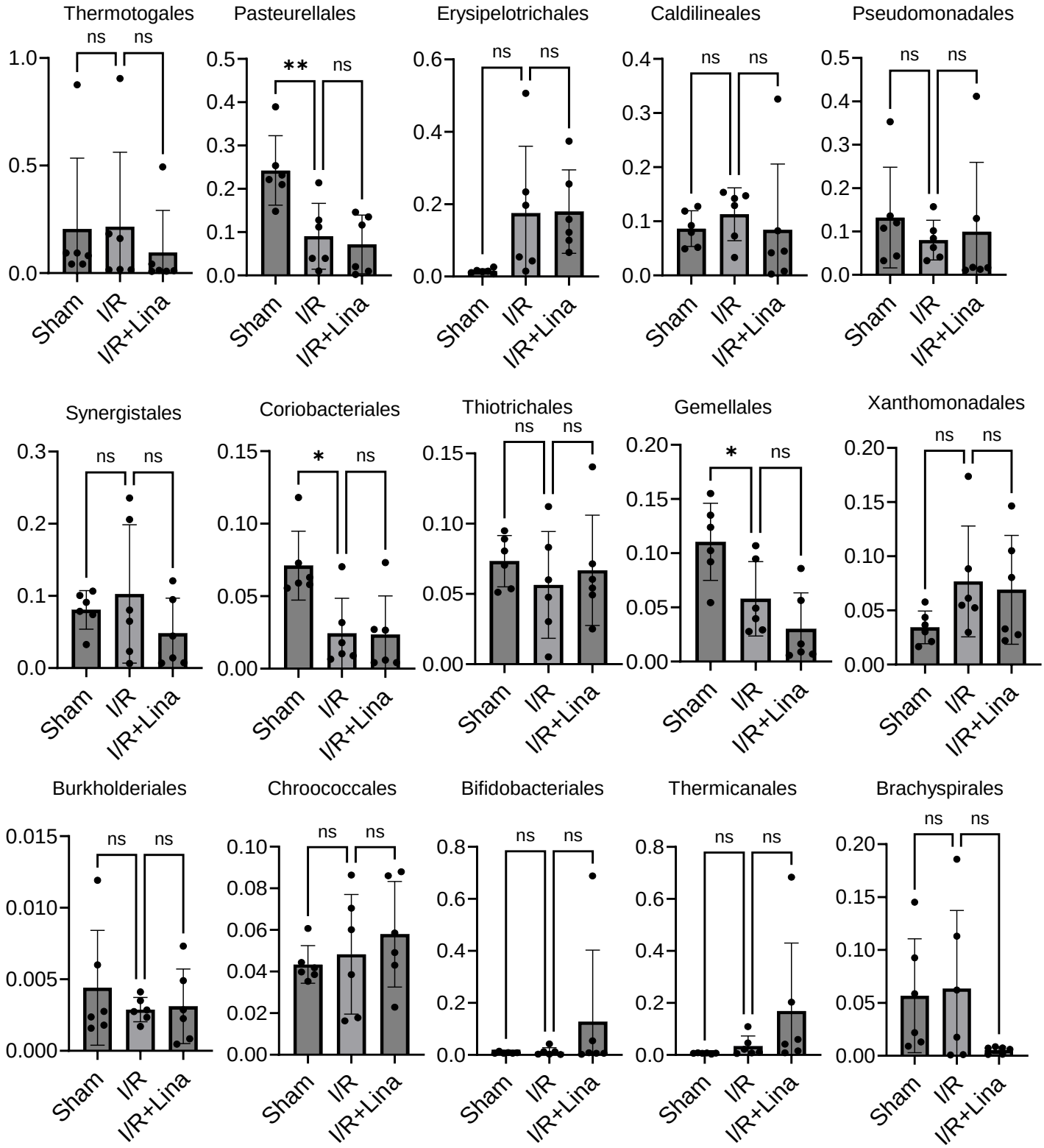

Supplementary Fig.S2
Order taxa

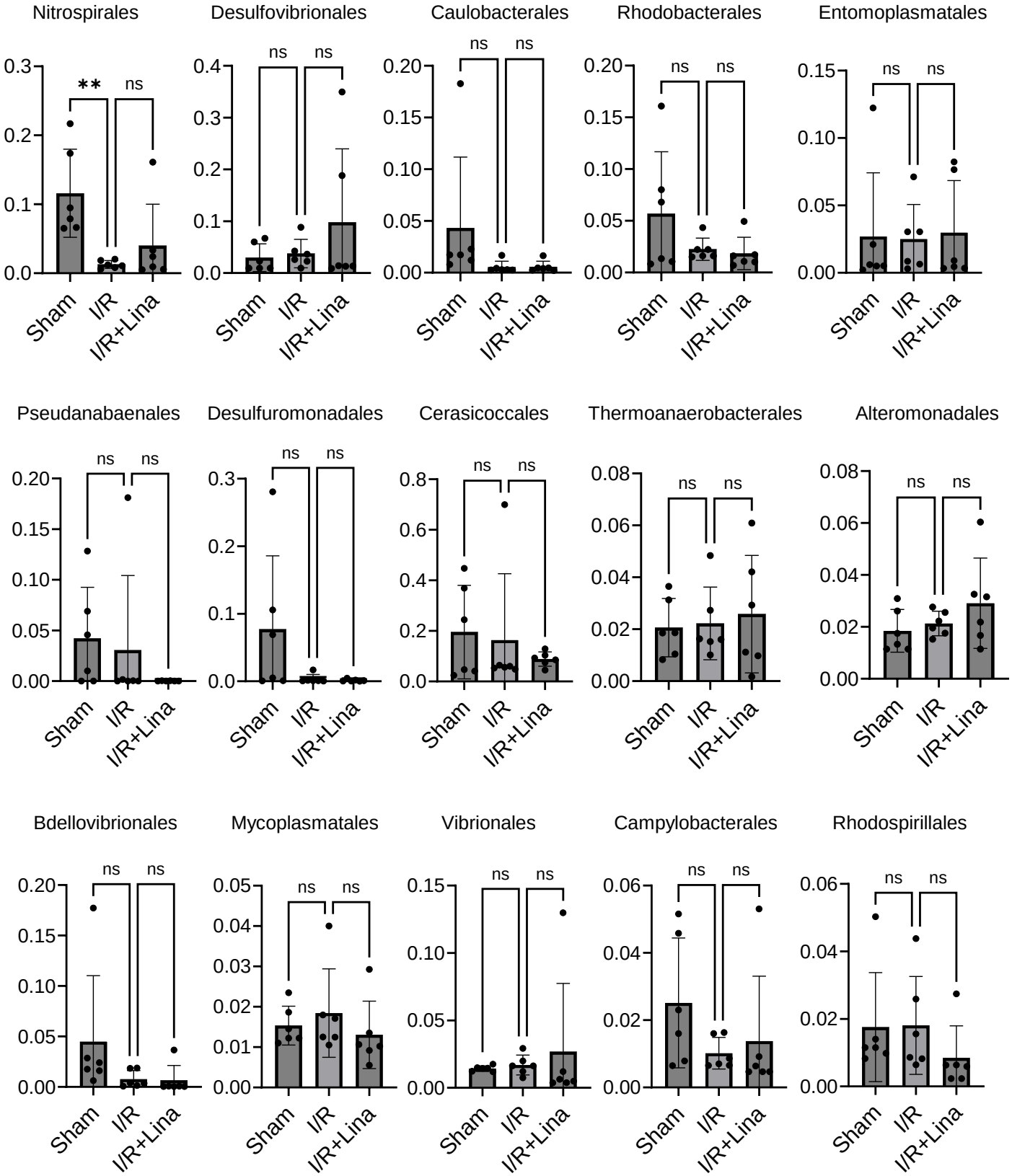

Supplementary Fig.S2
Order taxa

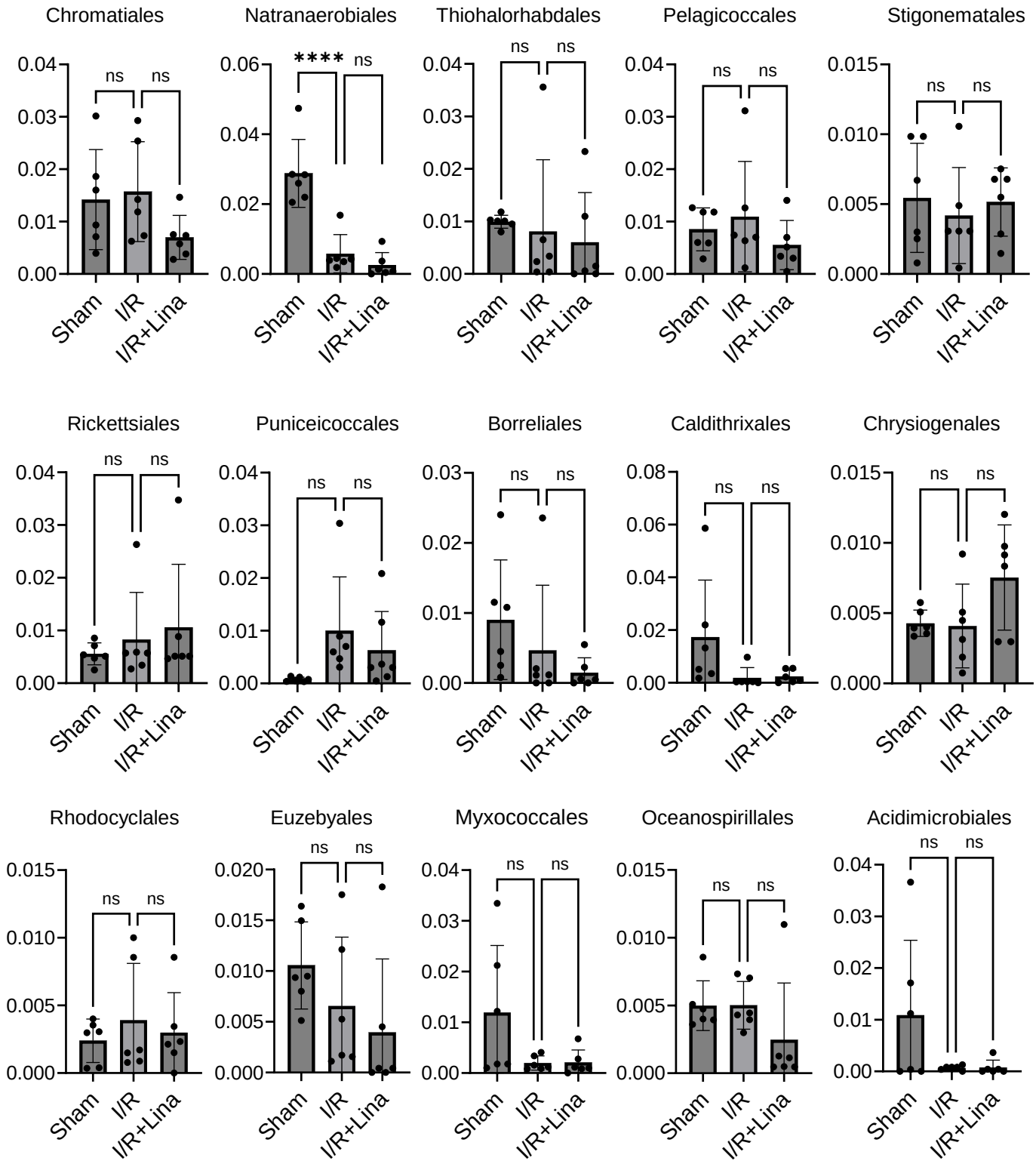

Supplementary Fig.S2
Order taxa

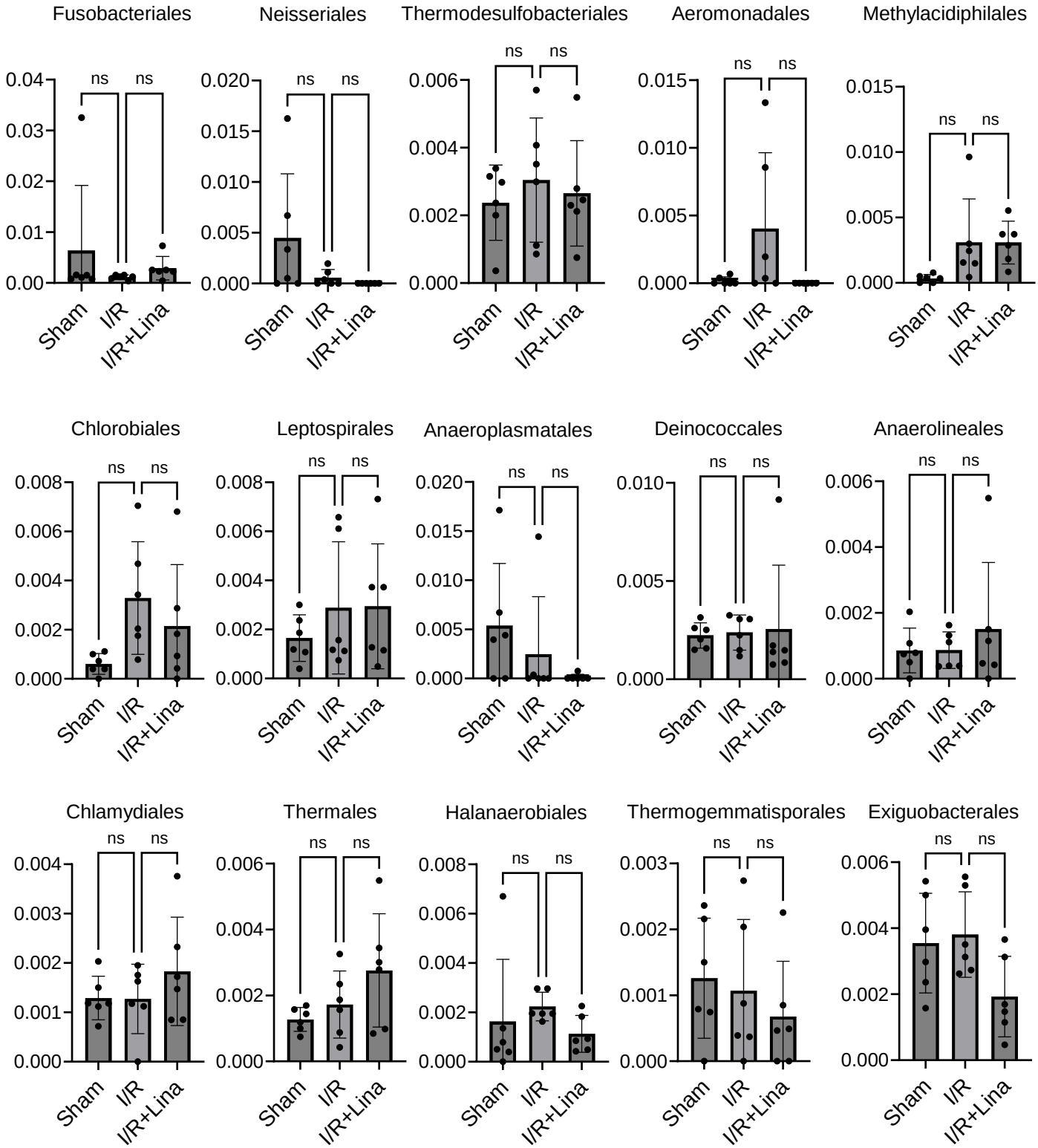

Supplementary Fig.S2
Order taxa

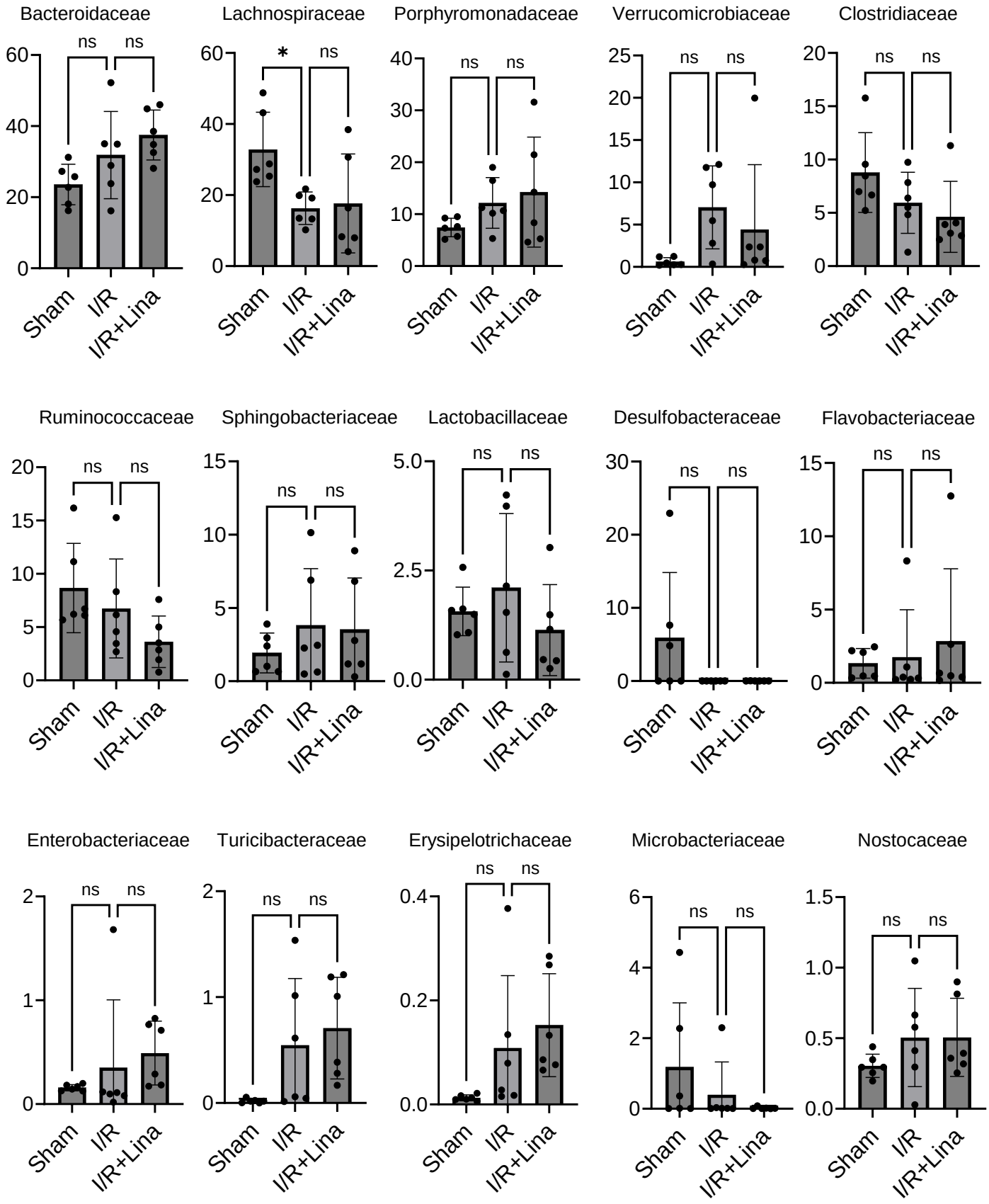

Supplementary Fig.S3
Family taxa

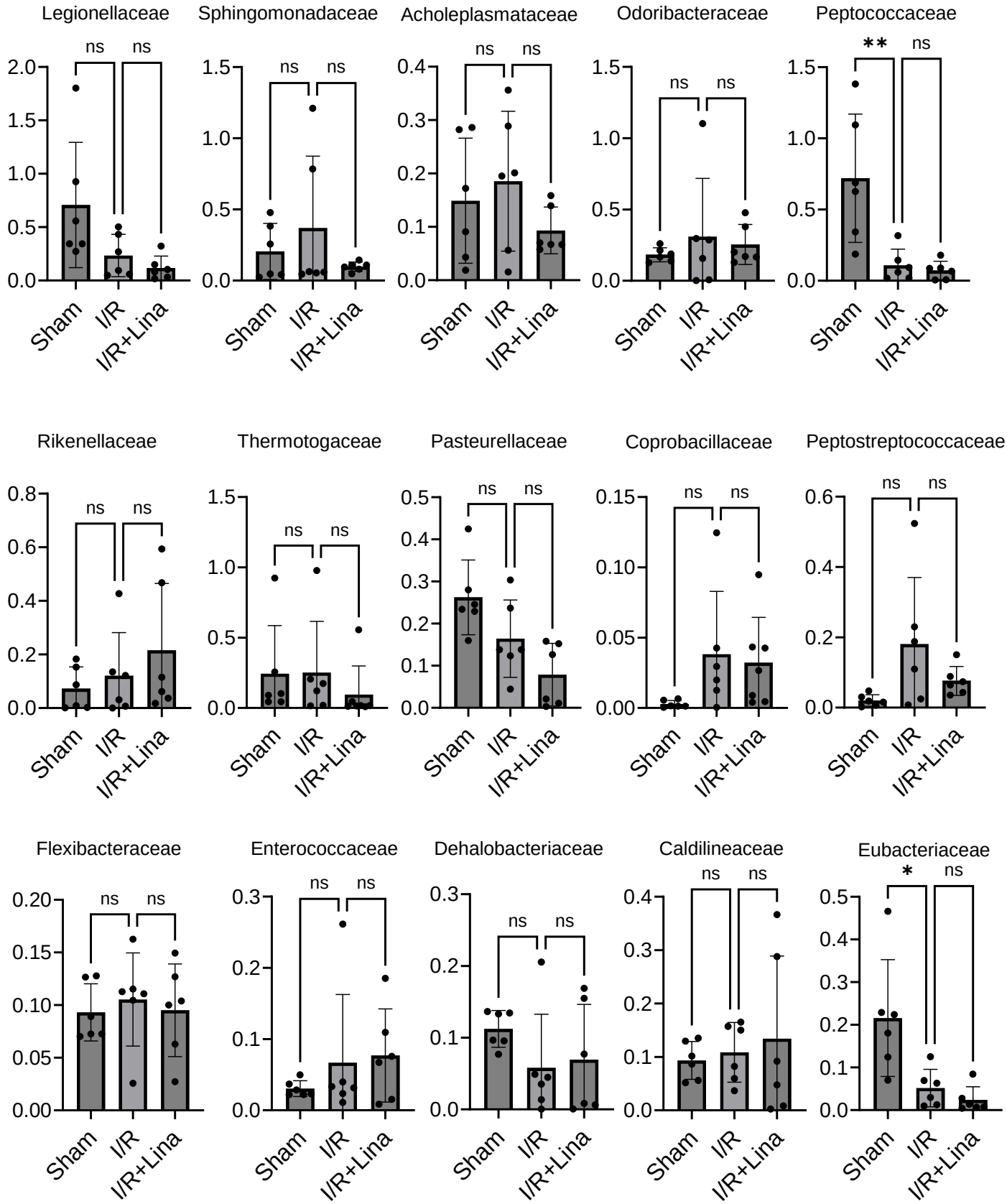

Supplementary Fig.S3
Family taxa

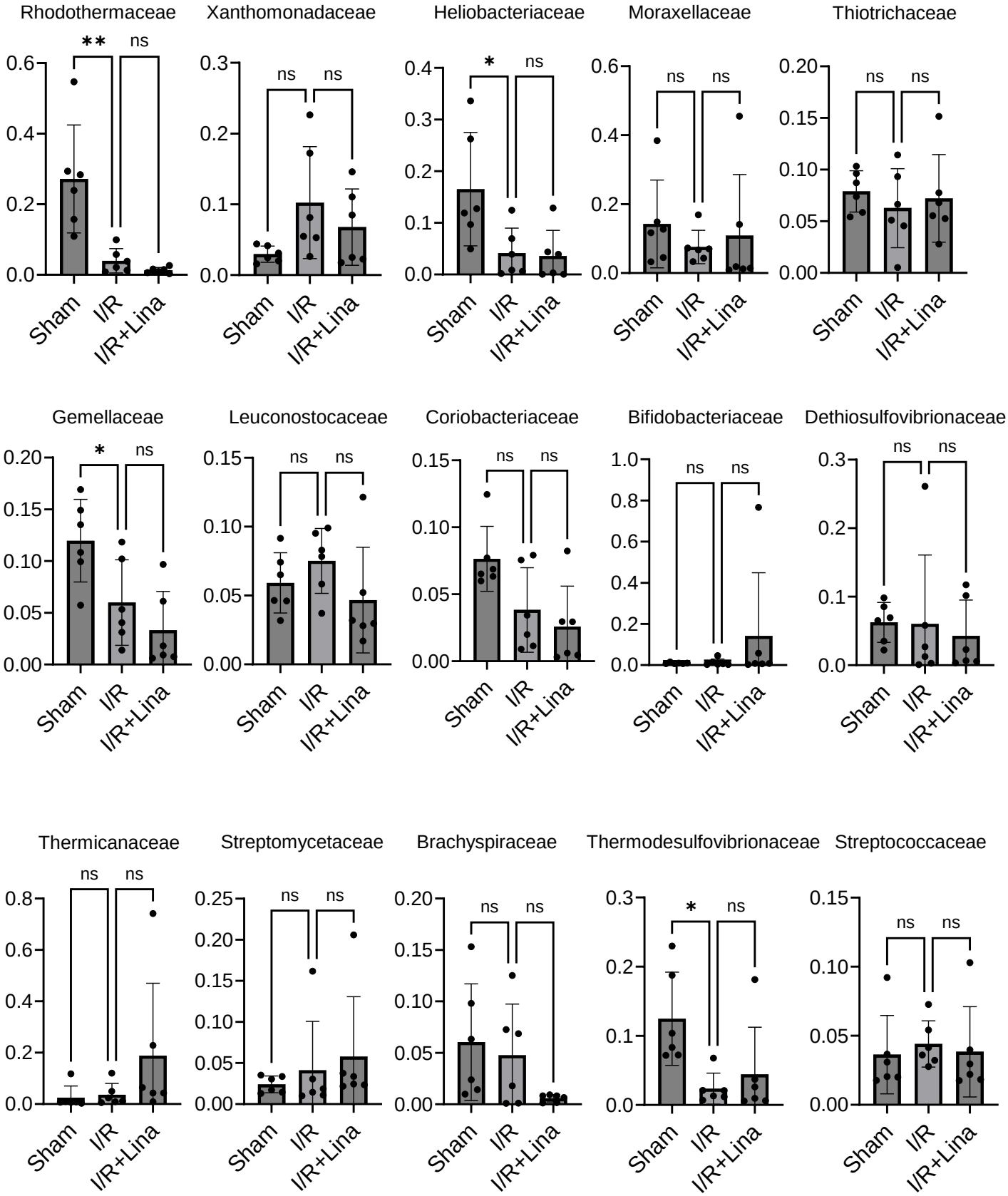

Supplementary Fig.S3
Family taxa

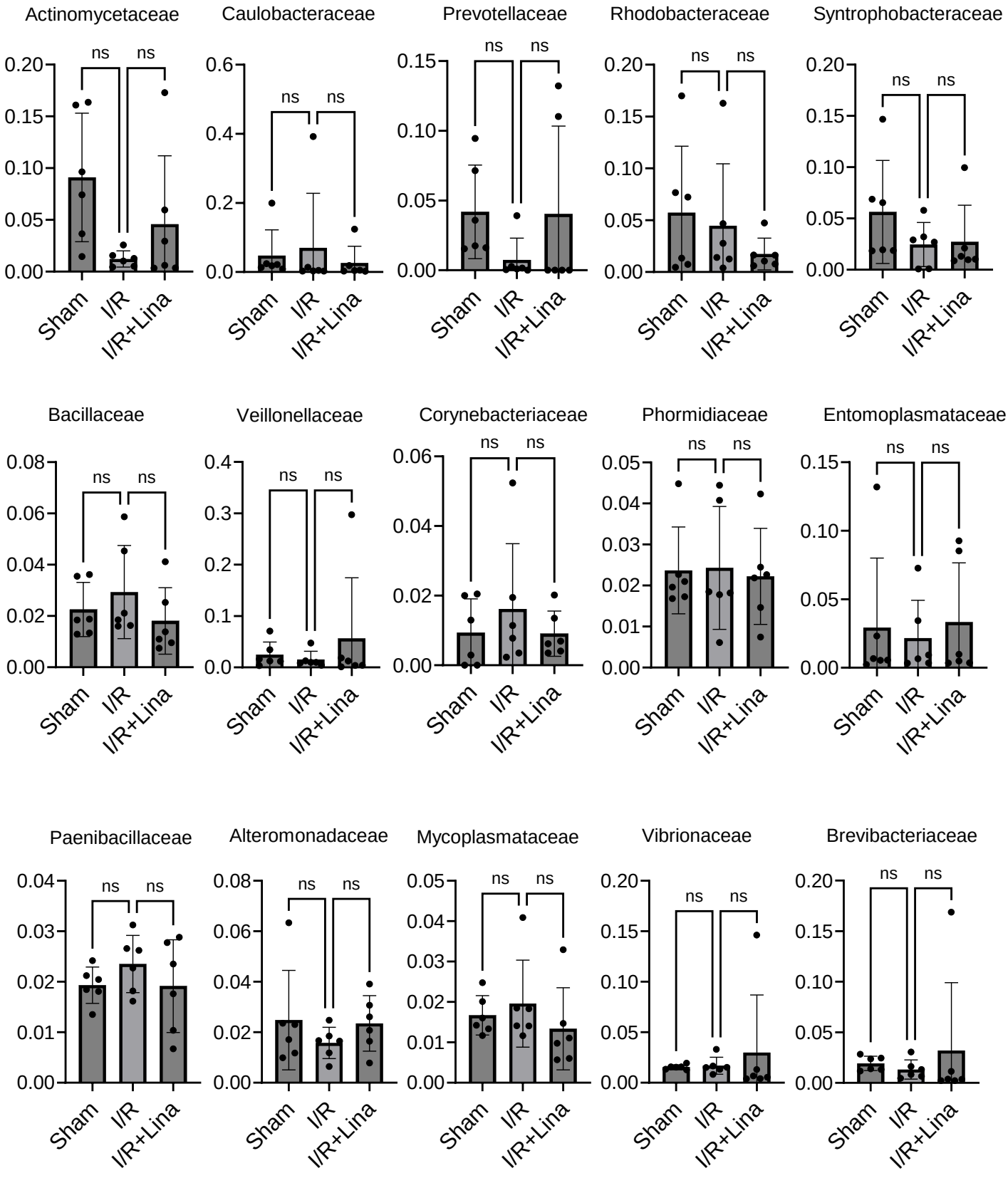

Supplementary Fig.S3
Family taxa

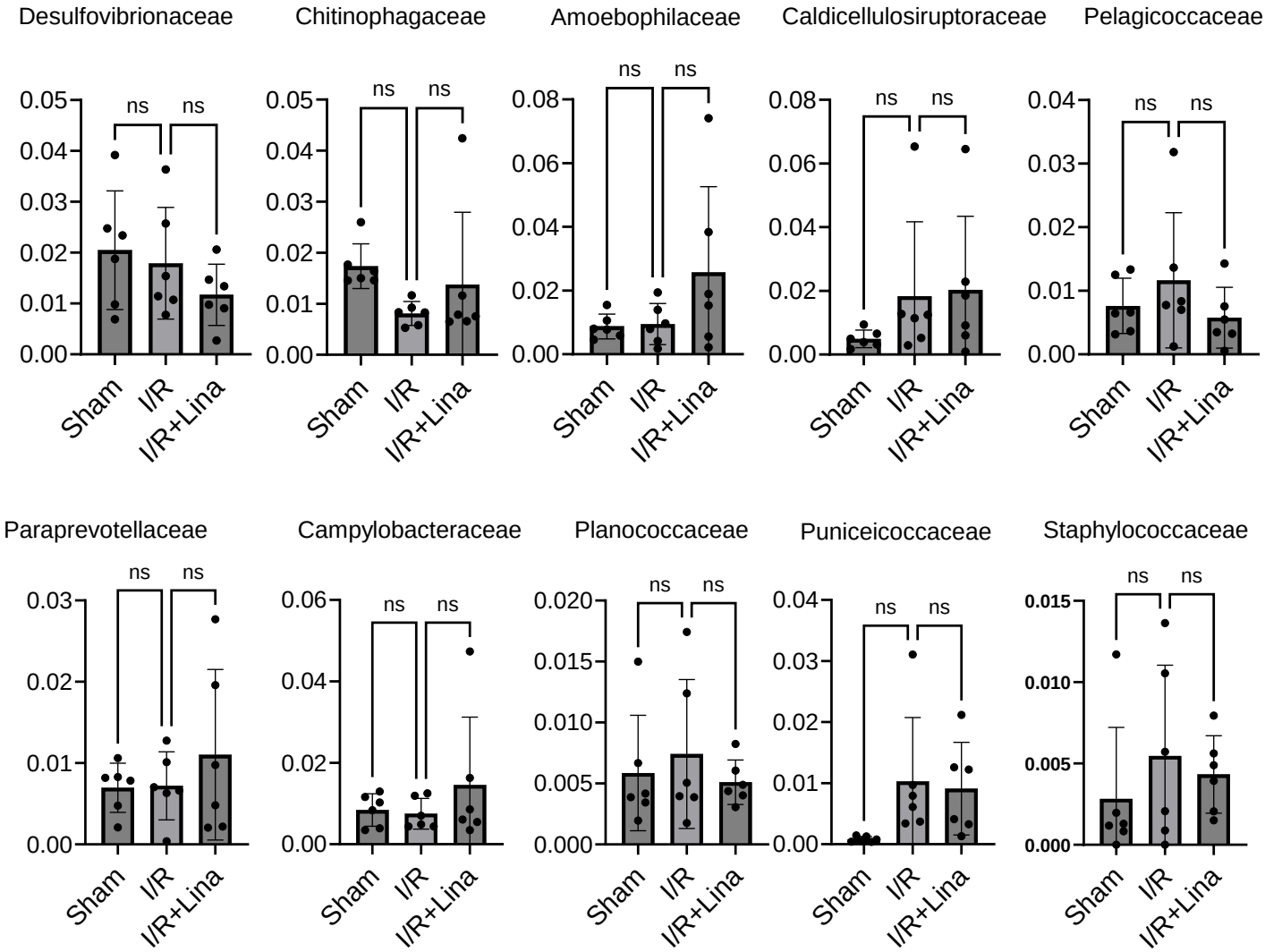

Supplementary Fig.S3
Family taxa

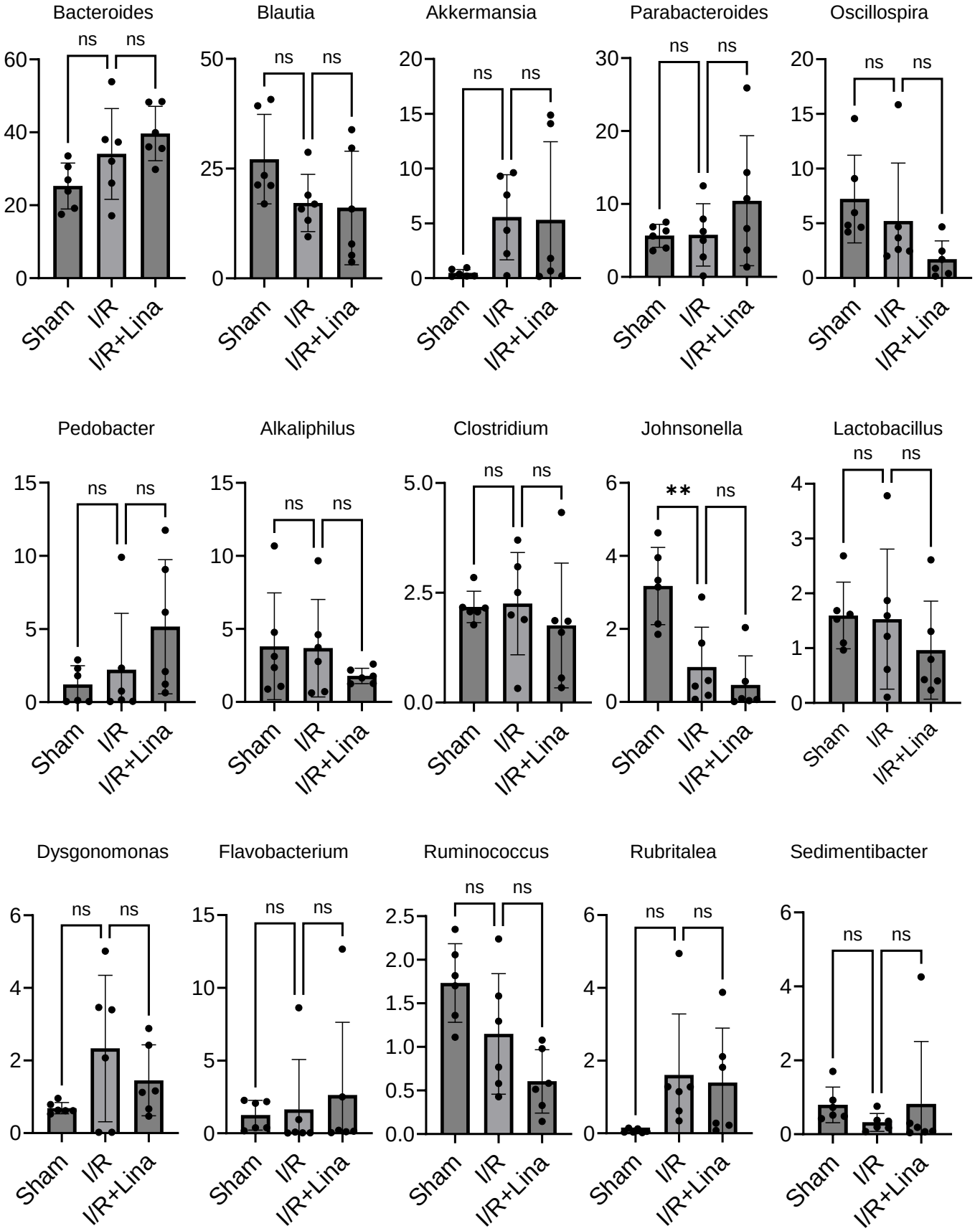

Supplementary Fig.S4
Genus taxa

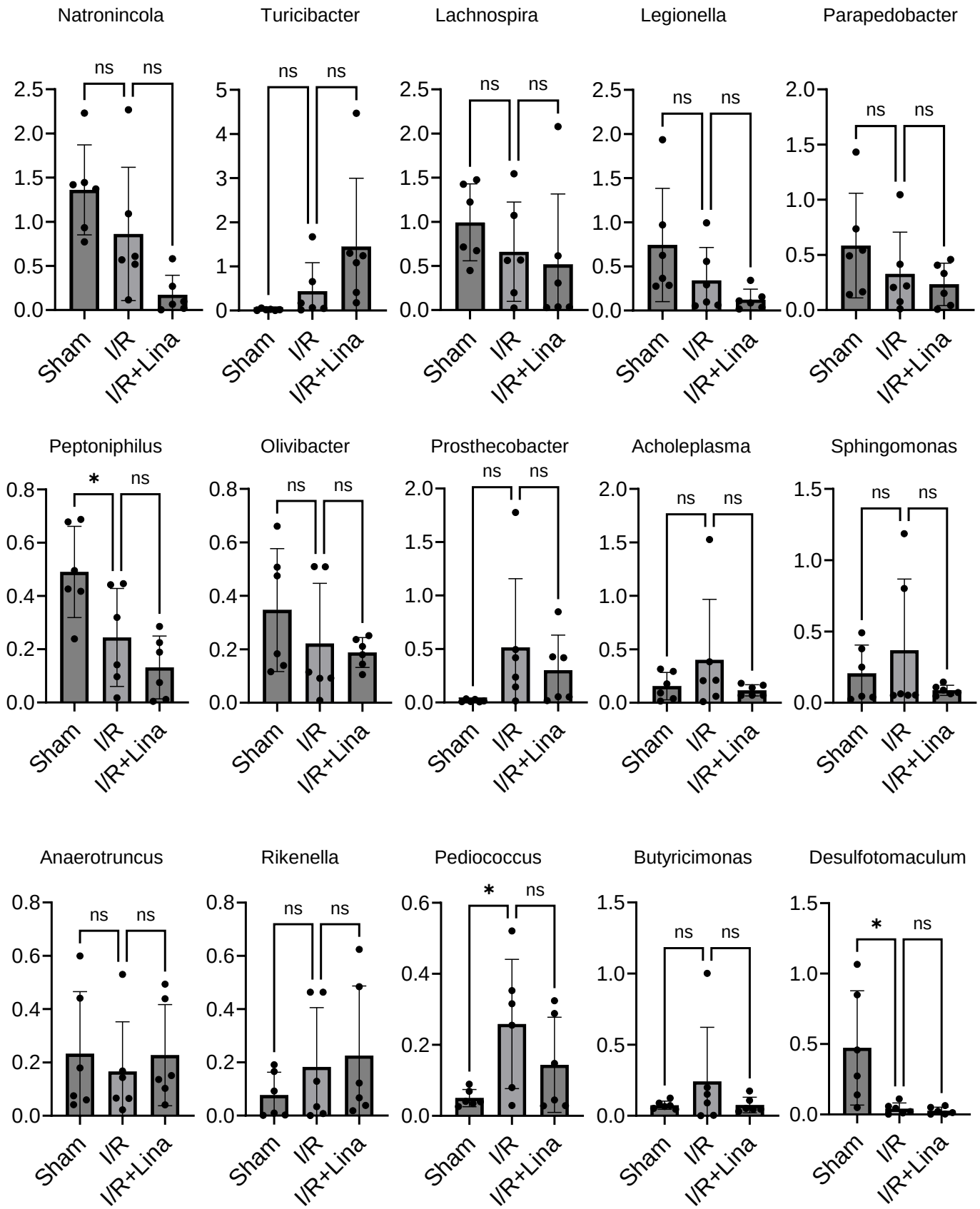

Supplementary Fig.S4
Genus taxa

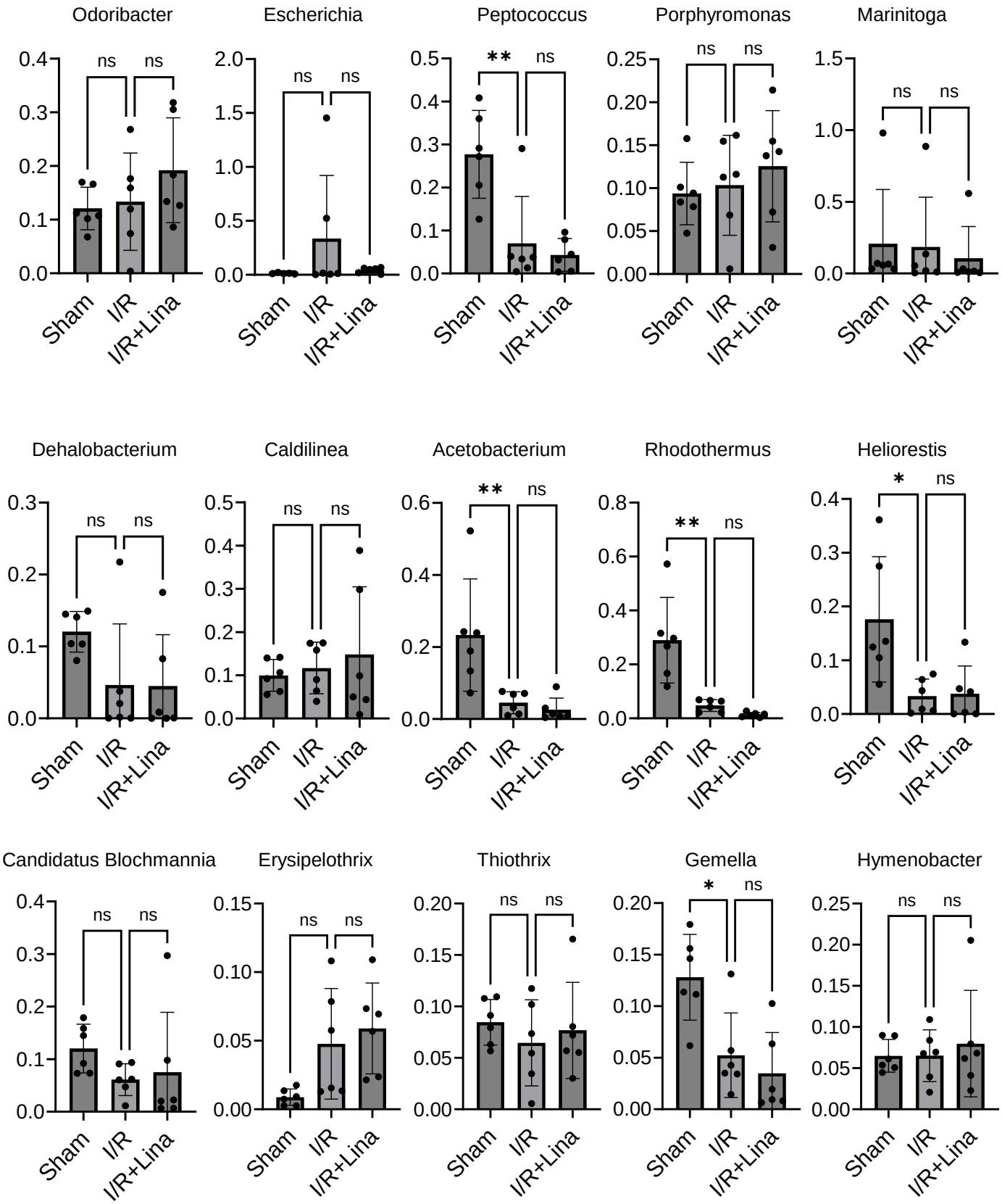

Supplementary Fig.S4
Genus taxa

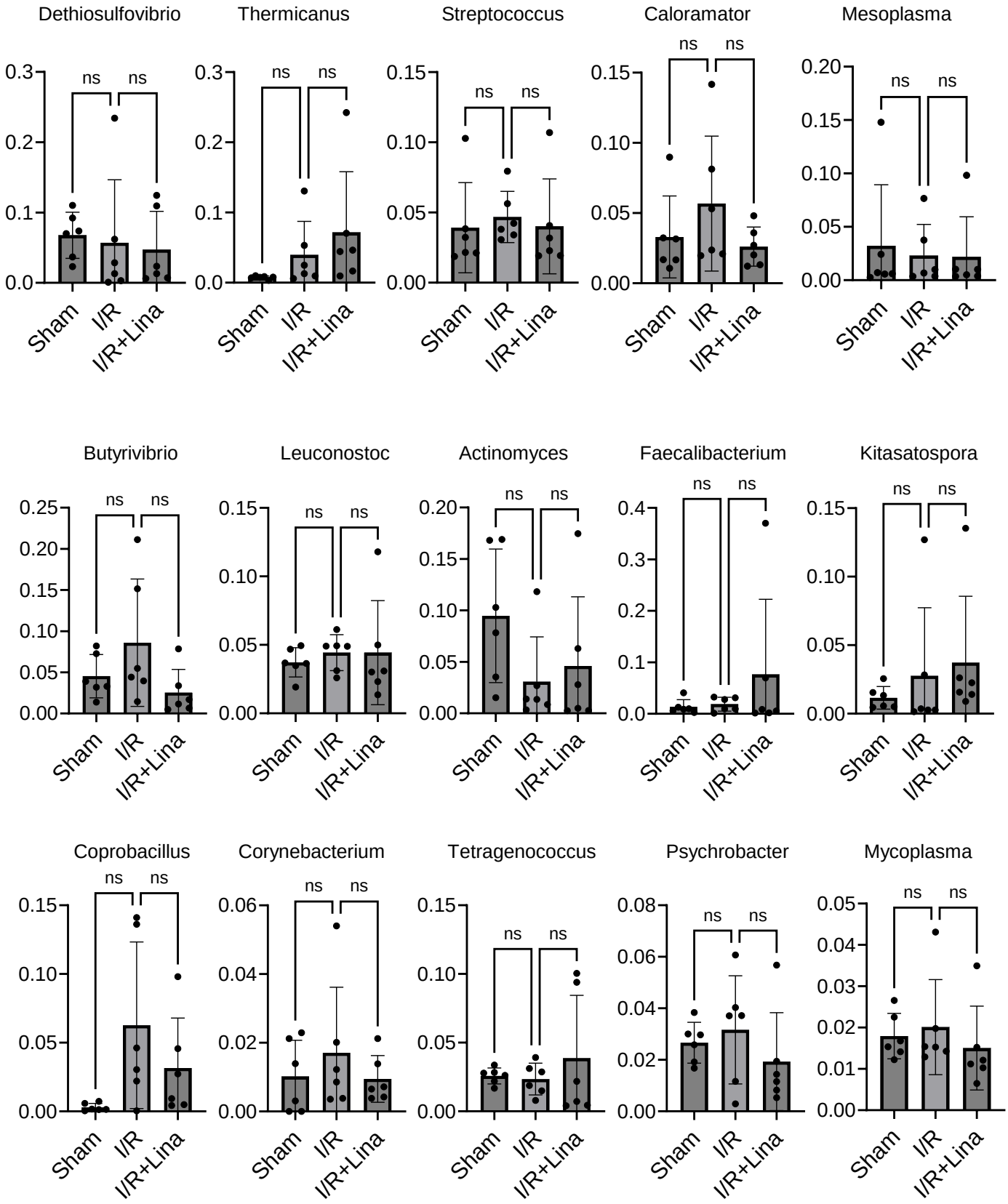

Supplementary Fig.S4
Genus taxa